ORIGINAL RESEARCH ARTICLES

DESIGNING, SYNTHESIS AND BIOLOGICAL EVALUATION OF PYRAZOLINE DERIVATIVES TARGETING PANCREATIC CANCER CELLS

Sarita S. Shinkar[a], Sarvanti R. Bhairi[a], Priyanka M. Khedkar[b], Swati R. Dhande[b] and Deepali M. Jagdale[a]*

(Received 09 December 2022) (Accepted 18 August 2023)

ABSTRACT

In continuation of the previous work based upon pyrazoline derivatives having cytotoxic activity, twenty-one 1,3,5-substituted pyrazoline derivatives were designed taking into consideration the important functional groups of methisazone, sorafenib and chalcone. The designed derivatives were screened using a preliminary molecular docking simulation study for evaluation of their binding interactions with receptor-2 of vascular endothelial growth factor, i.e., PDB ID: 3WZD. The synthesized derivatives were biologically evaluated for *in vivo* anti-angiogenic activity using adult zebrafish, its embryo, and *in vitro* anti-proliferative activity against pancreatic cancer MIA-PA-CA-2 cell line using the sulforhodamine B assay. Compound **5b** emerged as a promising hit molecule as it manifested moderate *in vitro* cytotoxic activity. Besides, its ability to inhibit zebrafish caudal fin regeneration with less phenotypical changes in zebrafish embryos suggests its promising potential against pancreatic cancer by VEGFR-2 inhibition as a mode of action.

Keywords: VEGFR, zebra fish embryo, 3WZD, MIA PA CA 2 cell line, pancreatic cancer

INTRODUCTION

Pancreatic cancer is the fourth most common cause of cancer-related mortality in the world. The survival rate is less than 1 % in pancreatic cancer patients which is the lowest among all malignancies[1,2]. The reason for the aggressive behaviour of pancreatic cancer is its malignant nature, which causes the rapid spread of cancer to other parts of the body.

Targeted therapy is one of the most accepted approaches in the treatment of cancer. Amongst various targets in treating cancer, the Vascular Endothelial Growth Factor Receptor (VEGFR) inhibition might be an effective approach mainly due to the obvious vascularity of the tumour[3-5]. VEGF is an essential regulator of angiogenesis. Thus, various agents, i.e., VEGF-A blockers, antibodies for VEGFR-2, and VEGFR-2 kinase activity inhibitors, are widely studied. Ultimately, these agents can stop the new blood vessel growth in the tumor leading to tumor cell death[6-8]. It is well documented in clinical trial studies that VEGFR-targeted therapy has mainly delayed but does not shrink the tumor and hence is cytostatic, as was first hypothesized[9].

Marschall et al. have reported that for pancreatic cancer the VEGFR existence is important as an autocrine/paracrine mitogenic loop[10]. Hotz et al. performed *in vitro* and *in vivo* studies of TNP-470 for anti-pancreatic cancer via VEGF inhibition, wherein it significantly reduced the proliferation and cell viability of human pancreatic cell lines MIA-PA-CA-2, AsPC-1, and Capan-1, which have an abundant expression of VEGFR on their surface. In *in vivo* evaluation, it was found that TNP-470 reduced tumor growth and metastatic spread of pancreatic cancer in a mouse model[11]. Inhibition of VEGFR and EGFR by the drug vandetanib is being evaluated in clinical trials for various cancers[12]. The marketed drugs like sunitinib, sorafenib and axitinib, which are used in the treatment of kidney cancer, are proposed to inhibit the VEGFR-2 receptor. Looking into all the recent developments involving VEGFR as a target, it was decided to design and develop novel

[a] Department of Pharmaceutical Chemistry, Bharati Vidyapeeth's College of Pharmacy, Sector 8, C.B.D. Belapur, Navi Mumbai-400 614, Maharashtra, India

[b] Department of Pharmacology, Bharati Vidyapeeth's College of Pharmacy, Sector 8, C.B.D. Belapur, Navi Mumbai-400 614, Maharashtra, India

*For Correspondence: E-mail: jagdaledeepali5680@gmail.com

https://doi.org/10.53879/id.60.09.13805

entities that could have a potential role in pancreatic cancer treatment via VEGFR-2 inhibition.

Herein, the present work reports the synthesis, characterization, docking simulation study, *in vitro* cell inhibition study on pancreatic cancer cell lines, and *in vivo* antiangiogenic activity of some 3, 5-diaryl-4, 5-dihydro-1*H*-pyrazole-1-carbothioic acid amide and *N*-(2-(1-carbamothioyl-5-aryl-4, 5-dihydro-1*H*-pyrazol-3-yl) phenyl) acetamide derivatives.

MATERIALS AND METHODS

Designing of molecules

In the process of designing molecules, various previously reported anti-pancreatic cancer agents such as methisazone, sorafenib and others were studied. It was observed that some functional groups were common among all these agents. It was found that methisazone (Fig. 1a) showed anti-pancreatic cancer activity as a virtue of the thiosemicarbazone group[13]. Thiosemicarbazone of *N*-heterocyclic compounds has a low ϖ-electron density of the side chain, and the heterocyclic ring with a nitrogen atom might be a good donor of electron pair to the receptor. Also, thiosemicarbazide can easily fit within the receptor cavity[14].

Kiyoshi Okamoto et al. performed docking simulation studies of sorafenib (Fig.1a) and found that the amide nitrogen of sorafenib interacted with Cys 919, whereas the ureide nitrogen bound at Glu 885 and the ureide carbonyl group bound at Asp 1046 of VEGFR-2[15].

On the other hand, Yau-Hung Chen et al. found that chalcone (Fig. 1a) showed good anticancer activity via VEGFR inhibition[16].

In our previous research work[17], we synthesized various pyrazoline derivatives with good cytotoxic

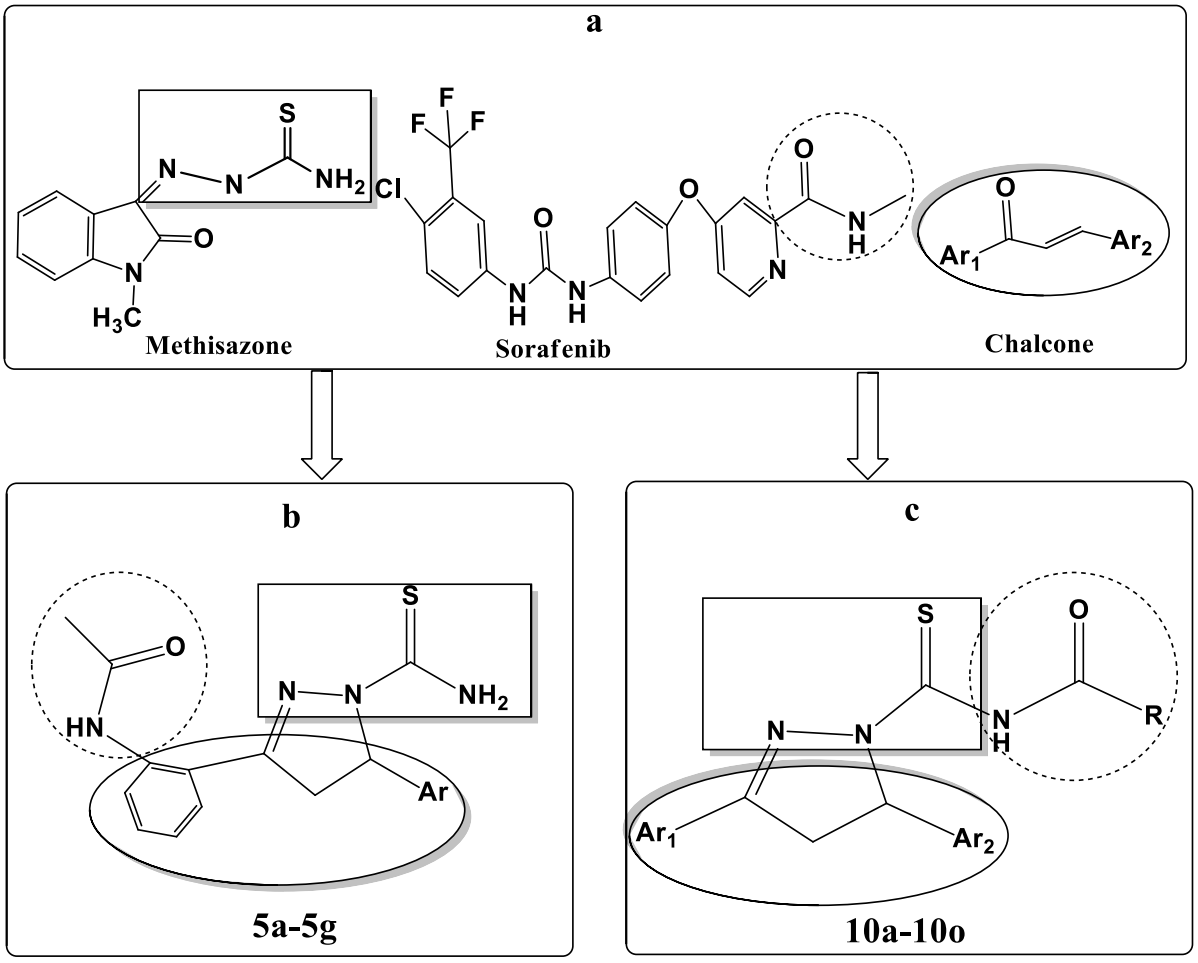

Fig. 1: Designing of novel pyrazoline derivatives as VEGFR-2 inhibitors;

a: Structures of methisazone, sorafenib and chalcone, **b:** Designed structure of *N*-(2-(1-carbamothioyl-5-aryl-4, 5-dihydro-1*H*-pyrazol-3-yl) phenyl) acetamide derivatives, **c:** Designed structure of 3, 5-diaryl-4, 5-dihydro-1*H*-pyrazole-1-carbothioic acid amide

activity. Also, the basic structural requirement of methisazone as shown in the square (Fig. 1) and an α, β- unsaturated carbonyl group of chalcone overlapping with the pyrazoline ring led us to molecules (Fig. 1b; 1c) being designed with pyrazoline as a scaffold, as shown in the oval shape. The amide functional group of sorafenib was included in **5a-5g** (Fig. 1b). The acyl group is attached to the thiosemicarbazone group in the designed compounds **10a–10o** (Fig. 1c), as indicated by the dashed circle.

Chemicals and physical characterization

All the reagents and the solvents were purchased from S. D. Fine Chem., Research Lab., and Sigma Aldrich, Mumbai, India. Analytical grade reagents were used. The solvents of commercial grade were purified before use. The completion of the reaction was monitored by means of thin layer chromatography (TLC) on silica gel coated aluminium sheets (Merck, Specialities Ltd., Mumbai, India). The compounds that could not be purified by means of recrystallization were subjected to flash chromatography for purification. Melting points were determined on a 'Veego' VMP-D melting point apparatus by the open capillary method and are expressed in ^{0}C. The FTIR spectra were recorded on a Shimadzu FTIR-8400S spectrophotometer using a potassium bromide pellet and are indicated in cm^{-1}. The λ_{max} of individual compounds was recorded on a Shimadzu UV-1800 dual-beam spectrophotometer. Individual methanolic solutions of compounds **[5a-5g, 10a-10o]** were scanned in the range of 200-400 nm using methanol as a blank. The Agilent Technologies 1200 series was used to determine the purity of compounds. EZChrom Elite software (Version 3.2.1) provided by the manufacturer was used for data acquisition. The liquid chromatographic system was carried out using a C18 column (250 x 4.6mm, 5µm particle size). The water used was ultrapure Type-II HPLC grade (18.2 MΩ) obtained from PURELAB Flex (ELGA). Water was used after filtering through a 0.45 µm nylon membrane filter with sonication for 30 mins. The trace elements of 1H NMR spectra were recorded on a Varian spectrometer (400 MHz) at the Sophisticated Analytical Instrumental Facility (SAIF), University of Punjab, Chandigarh, India and Bruker Avance II (400 MHz) spectrometer at SAIF Laxai-Avanti Life Science where tetramethylsilane (TMS) served as an internal standard and deuterated chloroform ($CDCl_3$) as the solvent. Mass spectra were recorded on an Agilent 1100 spectrometer using the (ESI) technique at Laxai-Avanti Life Sciences Pvt. Ltd., Hyderabad, India.

The compound was added into the media containing embryos and was evaluated after 72 hpf (hour post

Table I: Chemical structures of synthesized (pyrazoline) derivatives

Compound	Ar	Compound	Ar_1	Ar_2	R
5a	$-C_6H_5$	10a	$-C_6H_5$	$-C_6H_5$	C_6H_5
5b	$-4ClC_6H_4$	10b	$-C_6H_5$	$-4BrC_6H_4$	C_6H_5
5c	$-4CH_3C_6H_4$	10c	$-C_6H_5$	$-4ClC_6H_4$	C_6H_5
5d	$-4BrC_6H_4$	10d	$-C_6H_5$	$4-(OCH_3)C_6H_4$	C_6H_5
5e	$-4FC_6H_4$	10e	$-C_6H_5$	$-4FC_6H_4$	C_6H_5
5f	$3,4-(OCH_3)_2C_6H_3$	10f	$-C_6H_5$	$-C_4H_3S$	C_6H_5
5g	$2,4-(Cl)_2C_6H_3$	10g	$-C_6H_5$	$-4CH_3C_6H_4$	C_6H_5
		10h	$-C_4H_3O$	$-4FC_6H_4$	C_3H_7
		10i	$-C_4H_3O$	$-4FC_6H_4$	CH_3
		10j	$-C_4H_3O$	$-4BrC_6H_4$	C_6H_5
		10k	$4-ClC_6H_4$	$-C_4H_3S$	C_3H_7
		10l	$4-ClC_6H_4$	$-C_4H_3S$	CH_3
		10m	$4-ClC_6H_4$	$-C_4H_3S$	C_6H_5
		10n	$4-ClC_6H_4$	$-4FC_6H_4$	C_3H_7
		10o	$4-ClC_6H_4$	$-4ClC_6H_4$	C_3H_7

fertilization) for abnormal phenotypes, i.e., abnormal vasculature, abnormal yolk sac, delayed hatching, hemorrhage, pericardial edema, and tail bending. The maximum phenotype changes were observed with embryos treated with 1.07 µg of compound **10b** followed by 0.53 µg of compound **5d** in a dose dependent manner. Phenotype changes in compound **5b** and **10l** treated embryos were observed in a non-dose dependent manner.

General synthetic procedure for chalcones: A suspension of o-amino acetophenone **1** (40 mmol) and aromatic aldehyde **2** (40 mmol) in ethanolic sodium hydroxide (NaOH) was stirred continuously for 4 h at a temperature ranging from 15-25 °C. The obtained reaction mixture was immediately poured into cold water to precipitate out the solid compound. The obtained compound was recrystallized with ethanol or acetone to obtain pure chalcone **3**[18].

The general method for synthesis of *N*-acetamide derivatives: Chalcone **3** (1 mmol) was refluxed with acetic anhydride (2 mL) for 30 mins. The reaction mixture was allowed to cool to room temperature and then poured into ice-cold water with vigorous stirring. The obtained precipitate was recrystallized using ethanol[19].

General method of synthesis of *N*-(2-(1-carbamothioyl-5-aryl-4,5- dihydro-1*H*-pyrazol-3-yl)phenyl)acetamide derivatives (5a-5g): Under stirring, *N*-acetamide derivative **4** (1 mmol) and thiosemicarbazide (3 mmol) were refluxed with ethanol (70 mL) till the complete dissolution of reactants occurred, i.e., for approximately 1 to 2 h. Under the same refluxing conditions, a solution of KOH (20 mmol) was added dropwise in ethanol (70 mL) followed by refluxing for 16 h. The reaction mixture was cooled at room temperature with overnight stirring to obtain a precipitate, which was further filtered under vacuum. Recrystallization was carried out with acetone or ethanol[20].

General synthetic procedure for *N*-thiocarbamoylpyrazole derivatives: The chalcone **8** (10 mmol), thiosemicarbazide (20 mmol), and ethanol (70 mL) mixture was refluxed with continuous stirring for approximately 1 to 2 h, so that the complete dissolution of reactants occurred. Under the same refluxing conditions, a solution of KOH (20 mmol) was dropwise added in ethanol (70 mL) and further refluxed for 7-8 h. The reaction mixture was then cooled and stirred overnight. Further, it was vacuum filtered. Recrystallization was carried out with acetone acetone or ethanol[20].

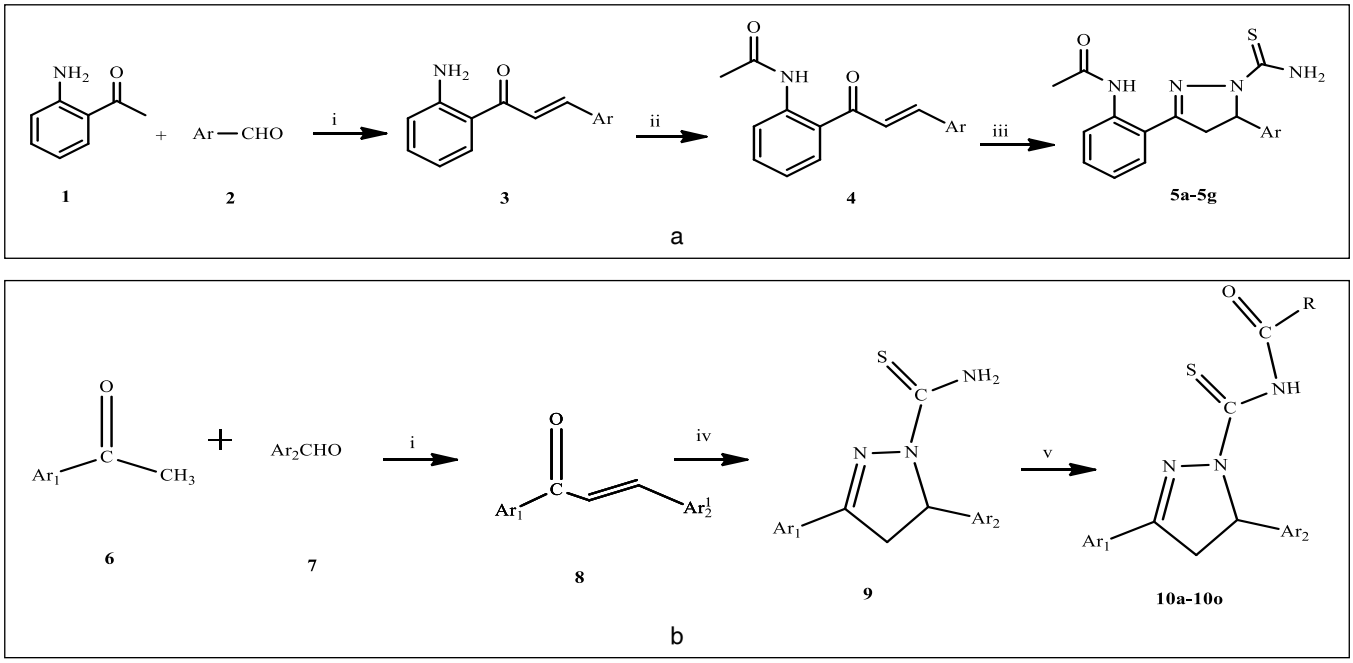

Scheme 1.a: Synthetic scheme of compounds 5a-5g. Reagents and conditions: - (i) Ethanolic sodium hydroxide solution, stir, 4 h; (ii) Acetic anhydride, reflux, 1 h; (iii) Thiosemicarbazide, ethanolic potassium hydroxide, reflux, 16 h; b:Synthesis of compounds 10a-10o.Reagents and conditions: - (i) Ethanolic sodium hydroxide solution, stir, 4 h; (iv) Thiosemicarbazide, ethanolic potassium hydroxide, reflux, 1 h; (v) Acetic anhydride, butyric anhydride, benzoic anhydride reflux, 1 h-5 h

General synthetic procedure for of *N*-benzoyl derivatives of 5-(aryl)-3-(phenyl)-4,5-dihydro-pyrazolo-1-carbothioic acid amide derivatives (10a-10o)

For 3-5 h, *N*-thiocarbamoylpyrazole derivative **9** (5 mmol) was refluxed with benzoic anhydride (1 g). The reaction mixture was allowed to cool to room temperature and then poured into ice-cold water with vigorous stirring. The precipitate obtained was re-crystallized using ethanol[19].

Preliminary molecular docking simulation studies

Docking studies have become an integral part of structure-based drug design. These studies help to predict to a certain extent, the affinity of the ligand for the receptor. All docking software are based on two main criteria: prediction of ligand and protein affinity and prediction of the correct pose of the ligand in the protein. Docking studies were performed by using the Maestro 10.1 module of Schrodinger software, installed on an Intel i3 processor running on the Windows 7 operating system. The crystal structure of VEGFR-2 was retrieved from the RCSB Protein Data Bank (PDB ID: 3WZD). Resolution: 1.57 Å with Lenvatinib as a ligand. Protein preparation was done by the Protein Prep wizard present in the software. All the water molecules bound to the protein were removed, missing residues were added, Het states were generated, and then minimization was carried out. After protein generation, grid generation was carried out in which the bound ligand, i.e., lenvatinib, was eliminated from the protein. Once the protein was prepared, the next step was to prepare ligands in their most stable configuration to achieve the most efficient docking studies. The structures of the compounds were modified by the LigPrep wizard, keeping the force field to OPLS_2005 using Epik mode. The maximum conformation was set to 100 and the minimum was set to 5. The docking was accomplished by the Glide docking module of the software, taking a grid size of 40, 40, and 40 Å (x, y, and z), keeping the scaling factor, and cutting off values to default as 0.8 and 0.15, respectively. The good binders were predicted in a large set with the top-scoring 10 % to 30 % using Glide extra precision (XP) docking available from Schrodinger. The set of conformers was generated in software for each ligand using the flexible docking mode. The extensive search to determine the possible positions and orientations of the ligand over the active site was then evaluated. The hierarchical filters like hydrogen bonding, docking score, and docking energy were set for the ligand poses to evaluate the interaction between the ligand and the receptor. The shortlisted ligand poses were subjected to further exposure to energy minimization on pre-computed van der Waals and electrostatic grids for the receptor. Thus, the final scoring was carried out on the poses which minimized the energy[23].

In vitro anticancer evaluation on cell line MIA-PA-CA-2

All the synthesized compounds were submitted to Tata Memorial's Advanced Centre for Treatment, Research, and Education in Cancer, Navi Mumbai, India, for performing their *in vitro* anticancer assay on Human pancreatic cancer cell line MIA-PA-CA-2. The protein binding dye i.e., sulforhodamine B was used.

Anti-angiogenic activity evaluation in zebrafish

The synthesized pyrazoline derivatives, which have shown better cell growth inhibition activity **(5b, 5d,** and **10l**) against *in vitro* cell line, were selected for screening anti-angiogenic activity.

Regenerative angiogenesis assay in adult zebrafish

To screen for the anti-angiogenic activity of these synthesized pyrazoline derivatives, the adult zebrafish (wild type) with approximately 1 g weight were utilized. A water tank with adequate aeration with 12 h light/dark light cycles was maintained. The fish were fed three times daily with micro pellets. They were kept for 15 days for acclimatization. The fish were divided into respective groups, with eight fish per group. The fish were anesthetized by using 2-phenoxy ethanol for the amputation of their fins with a sterile razor blade. The test compound was dissolved in 1 mL of DMSO and then added to the respective tank containing fish. Group one was for vehicle control (1 mL DMSO). Compound **5b** high dose (0.96/150 mg mL^{-1}) was in group two. The compound **5b** low dose (0.44/150 mg mL^{-1}) was in group three, the compound **5d** high dose (0.20/150 mg mL^{-1}) was in group four, the compound **5d** low dose (0.09/150 mg mL^{-1}) was in group five, and the compound **10l** high dose (0.44/150 $mgmL^{-1}$) was in group six. The fish were exposed to the test compounds on alternate days, for 15 days. On the 7th day Post amputation (DPA), the images were captured using a Motic digital microscope (4X) to observe the growth of the caudal fin[22].

Developmental angiogenesis assay in adult zebrafish

To determine the *in vivo* angiogenesis inhibition, zebrafish embryos were exposed to these pyrazoline

Table II: Physicochemical properties and spectroscopic structural characterization of compounds 5a-5g

Comp.	Physicochemical properties			Spectroscopic chemical structural characterization					
	Yield (%)	MP (^{0}C)	UV λ_{max} (nm)	MS (m/z)	FTIR (cm^{-1})	^{1}H-NMR (400 MHz, DMSO)			
						δ ppm	No. of protons	Splitting	Assignment
5a	64.88	238	315	339 M^++1	3433: NH, 3371, 3327: NH_2, 3032: Ar-H, 1678: C=O, 1593: C=N, 1066: C=S	10.4214	1H	s	NH
						8.1686-7.1868	10H	m	Ar-H
						8.0132	2H	bs	NH_2
						5.9024-5.9392	1H	dd	H_x
						3.9958-4.0690	1H	dd	H_b
						3.1527-3.2056	1H	dd	H_a
						2.1993	3H	s	CH_3
5b	66.5	229	315	373.1 M^++1	3464: NH, 3331, 3371: NH_2, 3030: Ar-H, 1687: C=O, 1583: C=N, 1185: C=S, 651: C-Cl	10.3842	1H	s	NH
						8.1926-7.1675	8H	m	Ar-H
						7.9982	2H	bs	NH_2
						5.9100-5.9475	1H	dd	H_x
						3.9891-4.0626	1H	dd	H_b
						3.1615-3.2150	1H	dd	H_a
						2.2128	3H	s	CH_3
5c	65	236	314	353.2 M^++1	3356: NH, 3232, 3267: NH_2, 2941: Ar-H, 1681: C=O, 1585: C=N, 1184: C=S	10.4221	1H	s	NH
						7.5143	2H	bs	NH_2
						8.2432-7.0443	8H	m	Ar-H
						5.8505-5.8870	1H	dd	H_x
						3.9685-4.0415	1H	dd	H_b
						3.1281-3.1811	1H	dd	H_a
						2.2753	3H	s	CH_3
						2.1914	3H	s	Ar-CH_3

5d	59	231	316	415.1 M^+-2	3433: NH, 3259, 3164: NH_2, 3032: Ar-H, 1678: C=O, 1593: C=N, 1105: C=S	10.3667 8.1615-7.1737 8.0569 5.8802-5.9181 3.9927-4.0663 3.1599-3.2137 2.1956	1H 8H 2H 1H 1H 1H 3H	s m bs dd dd dd s	NH Ar-H NH_2 H_x H_b H_a CH_3
5e	58	241	314	353 M^++1	3437: NH, 3255, 3140: NH_2, 3066: Ar-H, 1678: C=O, 1585: C=N, 1157: C=S, 1006: C-F	10.4092 8.2080-7.0335 7.9642 5.9197-5.9568 3.9854-4.0588 3.1672-3.2202 2.2171	1H 8H 2H 1H 1H 1H 3H	s m bs dd dd dd s	NH Ar-H NH_2 H_x H_b H_a CH_3
5f	52.88	230	315	399.1 M^++1	3433: NH, 3269, 3167: NH_2, 3032: Ar-H, 1678: C=O, 1593: C=N, 1105: C=S	10.4480 8.1285-6.6716 7.9607 5.8616-5.8891 3.9502-4.0217 3.7627 3.1805-3.2247 2.2053	1H 7H 2H 1H 1H 6H 1H 3H	s m bs dd dd s dd s	NH Ar-H NH_2 H_x H_b $2(OCH_3)$ H_a CH_3
5g	54	221	315	407 M^++1	3460: NH, 3352, 3333: NH_2, 3066: Ar-H, 1670: C=O, 1585: C=N, 1165: C=S, 706: C-Cl	10.3152 8.1889-7.0344 8.1014 6.1205-6.1597 4.0538-4.1276 3.0869-3.1416 2.2174	1H 7H 2H 1H 1H 1H 3H	s m bs dd dd dd s	NH Ar-H NH_2 H_x H_b H_a CH_3

Table III: Physicochemical properties and spectroscopic structural characterization of compounds 10a-10o

Comp.	Physicochemical properties			Spectroscopic chemical structural characterization					
	Yield (%)	MP (^{0}C)	UV λ_{max} (nm)	MS (m/z)	FTIR (cm^{-1})	^{1}H-NMR (400 MHz, DMSO)			
						δ ppm	No. of protons	Splitting	Assignment
10a	71	146	297	386.1 (M^+)	3417: N-H, 3061: Ar-H, 1633: C=O, 1329: C-N, 1244: C=S	8.0191-7.2347 5.8033-5-8452 3.8223-3.7656 3.1808-3.2374	15H 1H 1H 1H	M dd dd dd	Ar-H H_x H_b H_a
10b	91	162	296	464.20 (M^+)	3306: N-H, 3047: Ar-H, 1637: C=O, 1329: C-N, 1070: C=S	8.0296-7.2612 5.7732-5.8156 3.7697-3.8434 3.1543-3.2112	14H 1H 1H 1H	m dd dd dd	Ar-H H_x H_b H_a
10c	60	144	297	420.1 (M^+)	3417: N-H, 3057: Ar-H, 1627: C=O, 1334: C-N, 1087: C=S	8.0111-7.3283 5.7735-5.8153 3.7647-3.8438 3.1546-3.2117	14H 1H 1H 1H	m dd dd dd	Ar-H H_x H_b H_a
10d	67	134	295	415.0 (M^+)	3417: N-H, 3057: Ar-H, 1622: C=O, 1246: C-N, 1180: C=S.	8.0214-6.8745 5.7624-5.8023 3.7715-3.7528 3.7345-3.8082 3.1782-3.2359	14H 1H 3H 1H 1H	m dd dt dd dd	Ar-H H_x O-CH_3 H_b H_a
10e	62	116	297	402.2 (M^+)	3417: N-H, 3059: Ar-H, 1629: C=O, 1296: C-N, 1157: C=S	7.0043-7.7216 5.7874-5-8294 3.7645-3.8382 3.1649-3.2216	14H 1H 1H 1H	m dd dd dd	Ar-H H_x H_b H_a

10f	83	142	296	394.30 (M^++2)	3417: N-H, 3053: Ar-H, 1629: C=O, 1240: C-N, 1132: C=S	7.9927-6.9371 6.1397-6.1797 3.7488-3.8214 3.3761-3.4315	12H 1H 1H 1H	m dd dd dd	Ar-H H_x H_b H_a
10g	63	141	297	400.1 (M^++1)	3429: N-H, 3057: Ar-H, 1620: C=O, 332: C-N, 1182: C=S	7.9011-7.3210 5.6814-5-9023 3.6033-3.8627 3.1203-3.1334 2.2342-2.3636	14H 1H 1H 1H 3H	m dd dd dd s	Ar-H H_x H_b H_a CH_3
10h	62	146	299	360 (M^++1)	3300: N-H, 3078: Ar-H, 639: C=O, 1229: C=S, 126: C-F, 786: C-S	9.8107 6.5679-7.6127 6.0145-6.0518 3.7616-3.8348 3.1254-3.1794 2.8775-2.9269 1.7091-1.7644 0.9712-1.0081	1H 7H 1H 1H 1H 2H 2H 3H	s m dd dd dd dt sextet t	NH Ar-H H_x H_b H_a CH CH CH
10i	73	158	301	331 (M^+-1)	3389: N-H, 3070: Ar-H, 1658: C=O, 215: C=S, 1141: C-F, 798: C-S	7.5677 6.5167-7.5638 5.5256-5.5666 3.6654-3.7393 3.0442-3.0998 2.3998	1H 7H 1H 1H 1H 3H	s m dd dd dd s	NH Ar-H H_x H_b H_a CH
10j	58	151	302	453 (M^+)	3315: N-H, 3080: Ar-H, 1600: C=O, 1323: C=S, 783: C-S, 698: C-Br	7.9928 6.4875-7.9747 5.7088-5.7508 3.6869-3.7608 3.0667-3.1237	1H 12H 1H 1H 1H	S m dd dd dd	NH Ar-H H_X H_b H_a

10k	78	132	299	392 (M^++1)	3303: N-H, 3119: Ar-H, 1656: C=O, 819: C-Cl, 709: C-S	9.810 6.9824-7.6678 5.8956-5.9347 3.6474-3.7201 3.2649-3.3192 2.6757-2.8048 1.6392-1.7580 0.9636-1.0005	1H 7H 1H 1H 1H 2H 2H 3H	s m dd dd dd dt sextet t	NH Ar-H H_x H_b H_a CH CH CH
10l	73	174	301	364.2 (M^++1)	3388: N-H, 3057: Ar-H, 1656: C=O, 1095: C=S, 732: C-S, 692: C-Cl	6.9348-7.6703 5.5256-5.5666 3.6658-3.7384 3.2891-3.3432 2.3934	7H 1H 1H 1H 3H	m dd dd dd s	Ar-H H_x H_b H_a CH
10m	63	144	302	425 (M^+)	3313: N-H, 3066: Ar-H, 1656: C=O, 1215: C=S, 829: C-Cl, 785: C-S	6.9598- 7.9615 6.1406-6.1809 3.7178-3.7905 3.3341-3.3897	12H 1H 1H 1H	m dd dd dd	Ar-H H_x H_b H_a
10n	59	142	308	419 (M^+)	3308: N-H, 3144: Ar-H, 1637: C=O, 1033: C=S, 744: C-S, 698: C-Cl	7.0272- 7.6778 5.9038-5.9462 3.7650-3.8401 2.9830-3.0399 2.7446-2.9161 1.7408-1.8038 1.0065-1.0434	8H 1H 1H 1H 2H 2H 3H	m dd dd dd dt sextet t	Ar-H H_x H_b H_a CH CH CH
10o	66	138	305	401.3 (M^+-1)	3244: N-H, 3078: Ar-H, 1639: C=O, 1087: C=S, 788: C-S, 692: C-Cl	6.9785-7.8637 5.5458-5.5874 3.6161-3.7508 3.0623-3.1185 2.7062-2.8112 1.6863-1.7423 0.9570-0.9941	8H 1H 1H 1H 2H 2H 3H	dd dd dd dd dt sextet t	Ar-H H_x H_b H_a CH CH CH

Table IV: Cell growth inhibition (mia-pa-ca-2 cell line), and docking scores of synthesised compounds (5a-5g and 10a-10o)

Compound	GI_{50}(μM)	GI_{50}(M)	log GI_{50}	Docking score
5a	70.5	70.5 x 10^{-6}	-4.15	-6.898
5b	61.2	61.2 x 10^{-6}	-4.21	-5.739
5c	>100	>100 x 10^{-6}	>-4	-6.630
5d	40.6	40.6 x 10^{-6}	-4.39	-5.890
5e	79.1	79.1 x 10^{-6}	-4.10	-7.243
5f	90.6	90.6 x 10^{-6}	-4.04	-6.068
5g	>100	>100 x 10^{-6}	>-4	-6.068
10a	67.1	67.1x10^{-6}	-4.17	-6.44
10b	>100	100x10^{-6}	>-4	-6.88
10c	75.85	75.9x10^{-6}	-4-11	-6.34
10d	79.85	79.6x10^{-6}	-4.09	-6.94
10e	66.43	66.4x10^{-6}	-4.17	-6.44
10f	66.61	66.6x10^{-6}	-4.17	-6.33
10g	70.91	70.9x10^{-6}	-4.14	-6.49
10h	100	100 x 10^{-6}	>-4	-5.319
10i	76.9	76.9 x 10^{-6}	-4.11	-5.852
10j	88	88 x 10^{-6}	-4.05	-6.287
10k	>100	>100 x 10^{-6}	>-4	-5.574
10l	61.4	61.4 x 10^{-6}	-4.21	-5.574
10m	68.9	68.9 x 10^{-6}	-4.16	-5.176
10n	94.5	94.5 x 10^{-6}	-4.02	-5.776
10o	31	31 x 10^{-6}	-4.50	-4.938
Adriamycin	<0.1	<0.1 x 10^{-6}	< -7	-
Lenvatinib	-	-	-	-11.059
Sorafenib	-	-	-	-6.717

Table V: Zebrafish caudal fin regeneration on day 7

	Length of regenerated fin (μm)						
	DMSO (Vehicle control)	**5b** (0.96mg/ 150mL water)	**5b** (0.44mg/ 150mL water)	**5d** (0.20mg/ 150mL water)	**5d** (0.09mg/150 mL water)	**10l** (0.44mg/ 150mL water)	**10l** (0.20mg/ 150mL water)
Dorsal	1806.5 ± 123.14	515.5 ± 85.36*	1267.6 ± 52.3*	929.4± 127.9*	1304.6± 78.25*	1167.6± 115.1*	1404.5± 103.83*
Cleft	1196.5± 114.7	386.4± 93.55*	766± 59.81*	448.2± 56.13*	609.6± 56.67*	487.5± 88*	632.8± 118.92*
Ventral	1659.5± 104.91	413.1± 82.44*	1256.6± 107.55*	945.7± 133.9*	1328.7± 69.04*	1081± 109.32*	1358.7± 107.57*

*n=8, where n is the number of fish per group. Values indicated are mean ± SEM of regenerated fin length in all groups on day 7. All values are expressed as mean±SEM, p<0.05, * indicates that there is a significant difference in values of Day 7 when compared to a control group using one-way ANOVA followed by Tukey's multiple comparison test.*

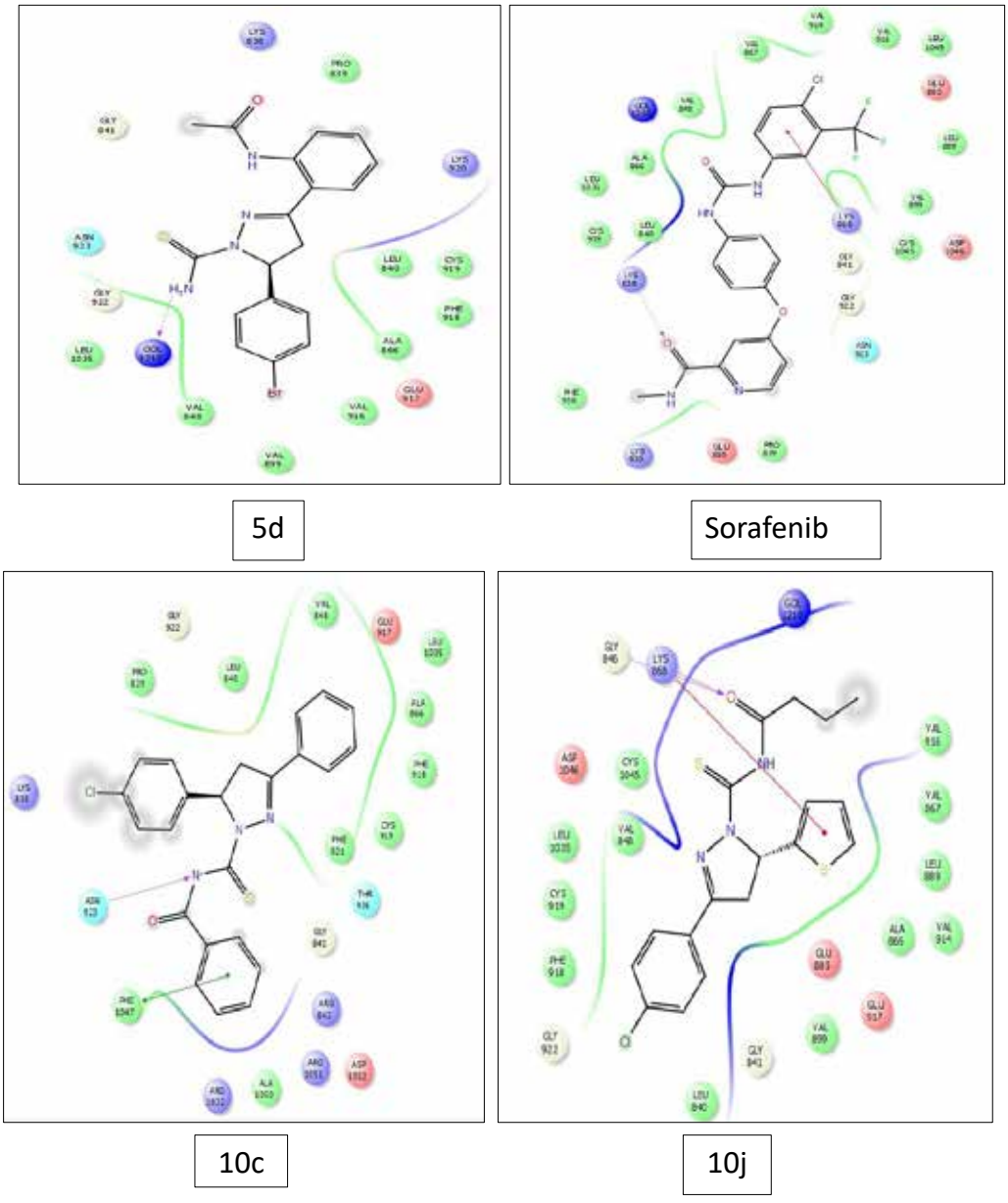

Fig. 2: Binding interactions of 5d, 10c, 10j, and reference drug sorafenib at VEGFR-2 (pdb id: 3wzd. Resolution: 1.57 å) generated by Schrodinger software

derivatives. The embryos were preserved in an embryo medium and divided into 17 groups. Group 1 was Vehicle control, group 2 was 1.07 µg of Compound **5b**, group 3 was 0.53 µg of Compound **5b** group 4 was 0.27 µg of Compound **5b**, group 5 was 0.13 µg of Compound **5b**, group 6 was 1.07 µg of Compound **5d**, group 7 was 0.53 µg of Compound **5d**, group 8 was 0.27 µg of Compound **5d**, group 9 was 0.27 µg of Compound **5d**, group 10 was 1.07 µg of Compound **10l**, group 11 was 0.53 µg of Compound 10l, group 12 was 0.27 µg of Compound **10l**, group 13 was 0.13 µg of Compound **10l**. The test compound was dissolved in DMSO and added to each well. The embryos were checked for various phenotypes after 72 hpf on a Motic digital microscope. The emergence of new phenotypical changes is an indication of an anti-angiogenic effect[22].

RESULTS AND DISCUSSION

Chemistry

The designed compounds were synthesized under simple laboratory conditions with more than 50 % yield. **Scheme 1** depicts the synthesis of pyrazoline derivatives (**5a-5g, 10a-10o**). 2-Amino acetophenone **(1, Scheme 1)**

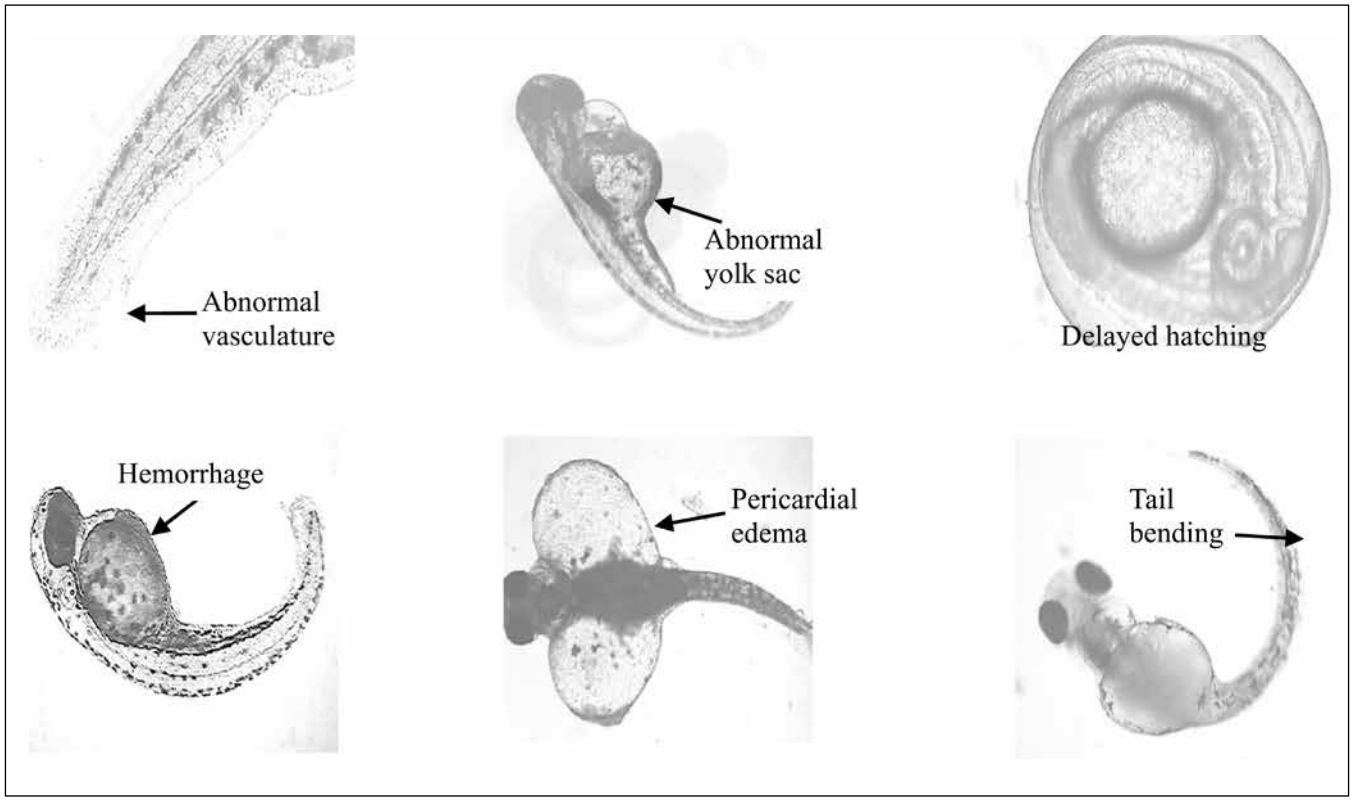

Fig. 3: Various phenotype changes observed in zebrafish embryo development at 72hpf

Table VI: Effect of compounds on phenotype changes in zebrafish embryos (72hpf)

Group	Phenotype changes					
	Tail Bending	Pericardial edema	Delayed hatching	Abnormal yolk sac	Abnormal vasculature	Total
1 (DMSO control)	0	0	0	0	0	0
2 (1.07µg of Compound **5b**)	0	6	7	0	0	13
3 (0.53µg of Compound **5b**)	0	5	5	3	2	15
4 (0.27µg of Compound **5b**)	2	4	4	4	3	17
5 (0.13µg of Compound **5b**)	6	2	3	4	4	19
6 (1.07µg of Compound **5d**)	0	7	5	5	2	19
7 (0.53µg of Compound **5d**)	1	6	5	7	2	21
8 (0.27µg of Compound **5d**)	2	6	4	5	2	19
9 (0.13µg of Compound **5d**)	2	3	2	3	1	11
10 (1.07µg of Compound **10l**)	0	4	9	0	0	13
11 (0.53µg of Compound **10l**)	0	4	7	0	0	11
12 (0.27µg of Compound **10l**)	2	3	3	3	2	13
13 (0.13µg of Compound **10l**)	2	2	1	4	1	10

n=12, where n is a number of embryos per group. Values indicate the number of embryos with phenotype changes in each group.

was used as a starting material to get chalcone **(3, Scheme 1),** which was further acylated to get the required amide functionality in derivatives **5a-5g** (Table I). Substituted acetophenones **(6, Scheme 1)** were reacted with thiosemicarbazide to get the required thiosemicarbazone structure (**10a-10o;** Table I). Table II (**5a-5g**) and Table III (**10a-10o**) show physiological properties and chemical characterization.

Docking simulation study

To confirm the interactions of the synthesized molecules with VEGFR-2, a preliminary docking simulation study was performed (Fig. 2). All the compounds as listed in Table I showed docking scores ranging from -5 to -7, which was similar to sorafenib. The docking scores were also in correlation with the GI_{50} values obtained from the *in vitro* cell growth inhibition study. As shown in Fig. 2, both the free amido group (**5d**) and the substituted amido group (**10c**) formed hydrogen bonds with the receptor, implying that both are structurally important in the molecules' activity. Looking at the docking score and docking interactions, it can be concluded that both the series (**5a–5g** and **10a–10o**) hold importance as VEFGR-2 inhibitors.

In vitro cell growth inhibition study on MIA-PA-CA-2 cell line

The synthesized compounds were evaluated for *in vitro* cell growth inhibitory activity against MIA-PA-CA-2 by using the sulforhodamine B assay at diverse concentrations to ascertain the GI_{50} values. The obtained GI_{50} values were converted to their log 10 and are reported. The $logGI_{50}$ values <-7 indicate the active compounds. $LogGI_{50}$ values >-7 to <-4 indicate moderately active compounds, whereas $logGI_{50}$ values of > -4 indicate inactive compounds (Table IV).

The observations in Table IV indicate that all the synthesized compounds except **5c**, **5g**, **10b**, **10h,** and **10k** exhibited moderate cell growth inhibition with $logGI_{50}$ values within the range of -7 to -4.

While designing the molecules, an attempt was made to include a thiosemicarbazide moiety in the pyrazoline ring with a free $-NH_2$ group (**5a-5g**), which is similar to methisazone, and an acetyl substituted $-NH_2$ group (**10a-10o**), which is similar to sorafenib. The results obtained from the *in vitro* cell growth inhibition study clearly indicate that the thioamide group, either free or substituted, did not cause much change in the activity of the molecules, i.e., the maximum molecules showed moderate cell growth inhibition. The substitution changes in the molecules did not affect the activity. The scaffold is more important for activity than that of substitutions.

Anti-angiogenic activity evaluation in zebrafish

Regenerative angiogenesis assay in adult zebrafish[21]

After the amputation of the caudal fin, the process of regeneration is started. During this, epithelial cell migration occurs to cover the wound, and regeneration blastema forms, followed by proliferation and differentiation of cells to replace the lost structure. For this study, an amputated fin was observed for fifteen days. From the study, it has been obtained that fish in the (vehicle control) group regenerate their caudal fin normally after fifteen days of amputation. The test compound treated group showed stunted growth of the caudal fin on the seventh day (Table V).

Developmental angiogenesis assay in zebrafish embryos

To determine the antiangiogenic potential of these compounds, the embryos were treated with four different concentrations. In zebrafish embryos, it usually takes up to 30 hpf to initiate circulation mainly in the major blood vessels i.e., inter-segmental, cardinal and sub-interstitial vessels[22].

The compounds were added into the media containing embryos and were evaluated after 72 hpf for abnormal phenotypes, i.e., abnormal vasculature, abnormal yolk sac, delayed hatching, hemorrhage, pericardial edema and tail bending (Fig. 3 and Table VI). The maximum phenotype changes were observed with embryos treated with 1.07 µg of compound **10b,** followed by 0.53 µg of compound **5d** which was dose dependent. While phenotype changes were seen in compound **5b** and **10l** treated embryos in a non-dose dependent manner.

CONCLUSION

N-(2-(1-carbamothioyl-5-aryl-4, 5-dihydro-1*H*-pyrazol-3-yl) phenyl) acetamide derivatives, (**5a-5g**) compounds having thioamide functional group similar to methisazone and 3, 5-diaryl-4, 5-dihydro-1*H*-pyrazole-1-carbothioic acid amide derivatives (**10a-10o)** having acyl group similar to sorafenib were designed and synthesized. The synthesized compounds were evaluated for *in vitro* cell inhibition study on MIA-PA-CA-2 cell line and *in vivo* anti-angiogenic activity on zebrafish and zebrafish embryos. All the compounds except **5c**, **5g**, **10b**, **10h,** and **10k** showed moderate *in vitro* cell inhibition. The *in vitro* results were comparable with docking simulation

study new results. Free amido group (**5a-5g**) as well as substituted amido group (**10a-10o**) showed hydrogen bond interaction with VEGFR-2 indicating that the thioamide group, either free or substituted, did not cause much change in the activity of the molecules. The compounds **5b**, **5d,** and **10l** showed significant anti-angiogenic activity in both regeneration and embryonal angiogenesis model in zebrafish. Out of these, **5b** showed regeneration of amputated fin length as 515.5 ± 85.36 µm, 386.4 ± 93.55 µm, 413.1 ± 82.44 µm, respectively, in the dorsal, cleft and ventral region of caudal fin in generational angiogenesis model and least phenotypes variation (13 phenotypes) in embryonic angiogenesis model, indicating the highest activity in comparison with all other compounds screened simultaneously. Thus, it can be concluded that compound **5b** has a potential as a good anticancer agent. Further, the active anticancer agents can be developed using **5b** as a scaffold.

ACKNOWLEDGEMENT

The authors would like to acknowledge Mr. Niranjan Mondal for contributing to this research work.

REFERENCES

1. Harsha H. C., Kandasamy K., Ranganathan P., Rani S., Ramabadran S., Gollapudi S. and et al.: A compendium of potential biomarkers of pancreatic cancer, **PLoS. Med**., 2009, 6(4), 18-24.
2. Iodice S., Gandini S., Maisonneuve P. and Lowenfels A. B.: Tobacco and the risk of pancreatic cancer: a review and meta-analysis, **Langenbeck's Arch. Surg**., 2008, 393(4), 535-545.
3. Prewett M., Huber J., Li Y., Santiago A., O'Connor W., King K. and, et al.: Antivascular endothelial growth factor receptor (fetal liver kinase 1) monoclonal antibody inhibits tumor angiogenesis and growth of several mouse and human tumors, **Cancer Res**., 1999, 59(20), 5209–5218.
4. Ciardiello F., Caputo R., Damiano V., Troiani T., Vitagliano D., Carlomagno F. and et al.: Antitumor effects of ZD6474, a small molecule vascular endothelial growth factor receptor tyrosine kinase inhibitor, with additional activity against epidermal growth factor receptor tyrosine kinase, **Clin. Cancer Res**., 2003, 9(4), 1546–1556.
5. Wedge S. R., Ogilvie D. J., Dukes M., Kendrew J., Curwen J. O., Hennequin L. F. and et al.: ZD4190: an orally active inhibitor of vascular endothelial growth factor signaling with broad-spectrum antitumor efficacy, **Cancer Res**., 2000, 60(4), 970–975.
6. Browder T., Butterfield C. E., Kraling B. M., Shi B., Marshall B., O'Reilly M. S. and et al.: Antiangiogenic scheduling of chemotherapy improves efficacy against experimental drug-resistant cancer, **Cancer Res**., 2000, 60(7), 1878–1886.
7. Escudier B., Eisen T., Stadler W. M., Szczylik C., Oudard S., Siebels M. and et al.: Sorafenib in advanced clear-cell renal-cell carcinoma, **New Engl. J. Med**., 2007, 356(2), 125–134.
8. Fujio Y. And Walsh K.: Akt mediates cytoprotection of endothelial cells by vascular endothelial growth factor in an anchorage-dependent manner, **J. Biol. Chem**., 1999, 274(23), 16349–16354.
9. Gerber H. P., McMurtrey A., Kowalski J., Yan M., Keyt B. A., Dixit V. and et al.: Vascular endothelial growth factor regulates endothelial cell survival through the phosphatidylinositol 3'-kinase/Akt signal transduction pathway. Requirement for Flk-1/KDR activation, **J. Biol. Chem**., 1998, 273(46), 30336–30343.
10. Marschall V. Z., Cramer T., Höcker M., Burde R., Plath T., Schirner M., and et al.: De novo expression of vascular endothelial growth factor in human pancreatic cancer: evidence for an autocrine mitogenic loop, **Gastroenterology**, 2000, 119(5), 1358-1372.
11. Hotz H. G., Reber H. A., Hotz B., Sanghavi P. C., Yu T., Foitzik T. and et al.: Angiogenesis inhibitor TNP-470 reduces human pancreatic cancer growth, **Gastrointest**. **Surg.**, 2001, 5(2), 131-138.
12. Morabito A., Piccirillo M. C., Falasconi F., De Feo G., Del Giudice A., Bryce J. and et al.: Vandetanib (ZD6474), a dual inhibitor of vascular endothelial growth factor receptor (VEGFR) and epidermal growth factor receptor (EGFR) tyrosine kinases: Current status and future directions, **Oncologist**, 2009, 14(4), 378-390.
13. Pelosi G.: Thiosemicarbazone metal complexes: From the structure to activity, **The Open Crystallography J.**, 2010, 3, 16-28.
14. Arora S., Agrawal S. and Singhal S.: Anticancer activities of thiosemicarbazides/thiosemicarbazones: A review, **Int. J. Pharm. Pharma. Sci.**, 2014, 9, 34-41.
15. Okamoto K., Kawada M., Jestel A., Konig K. V., Funahashi Y., Matsushima T., and et al.: Distinct binding mode of multikinase inhibitor lenvatinib revealed by biochemical characterization, **Med. Chem. Lett.**, 2014, 6(1), 89-94.
16. Chen Y., Chang C., Chang C., Chen P., Lee Y., Chern C. And et al.: Pro-angiogenic effect of chalcone derivatives in zebrafish embryos *in vivo*, **Molecules**, 2015, 20(7), 12512-12524.
17. Kharatmol M., Chavan P., Chavan R., and Jagdale D.: Study of *in vivo* antiangiogenic activity of novel pyrazoline derivatives by using zebra fish model, **World J. Pharm. Pharm. Sci.**, 2018, 7(5), 1454-1459.
18. Syam S., Abdelwahab S. I., Al-Mamary M. A., and Mohan S.: Synthesis of Chalcones with Anticancer Activities, **Molecules**, 2012, 17(12), 6179–6195.
19. El-Sabbagh O. I., Baraka M. M., Ibrahim S. M., Pannecouque C., Andrei G., Snoeck R. and et al.: Synthesis and antiviral activity of new pyrazole and thiazole derivatives, **Eur. J. Med. Chem.,** 2009, 44(9), 3746–3753.
20. Chimenti F., Carradori S., Secci D., Bolasco A., Bizzarri B., Chimenti P. and et al.: Synthesis and inhibitory activity against human monoamine oxidase of *N*1-Thiocarbamoyl-3,5-Di(hetero) aryl-4,5-dihydro-(1*H*)-pyrazole derivatives, **Eur. J. Med. Chem.**, 2010, 45(2), 800–804.
21. Jadhav V. M., Dhande S. R. and Kadam V. J.: Angiogenic effect of indigenous herbal extracts: *Bombax ceiba* and *Erythrina variegate*, **Ind. J. Nat. Prod. Resources**, 2018, 9(2), 126-131.
22. Bakkiyanathan A., Nathan J. R., Ravikumar S., Gopalakrishnan T. S., Aruldas F. M. and Malathi R.: Anti-angiogenic effects of theophylline on developing zebrafish (*Danio rerio*) Embryos, **Biomed. Prev. Nutr.**, 2012, 2 (3), 174–178.
23. https://www.schrodinger.com/science-articles/docking-and-scoring. Access Date- 24 September 2016.